# Figures and figure supplements

A translational MRI approach to validate acute axonal damage detection as an early event in multiple sclerosis

**Antonio Cerdán Cerdá and Nicola Toschi *et al*.**

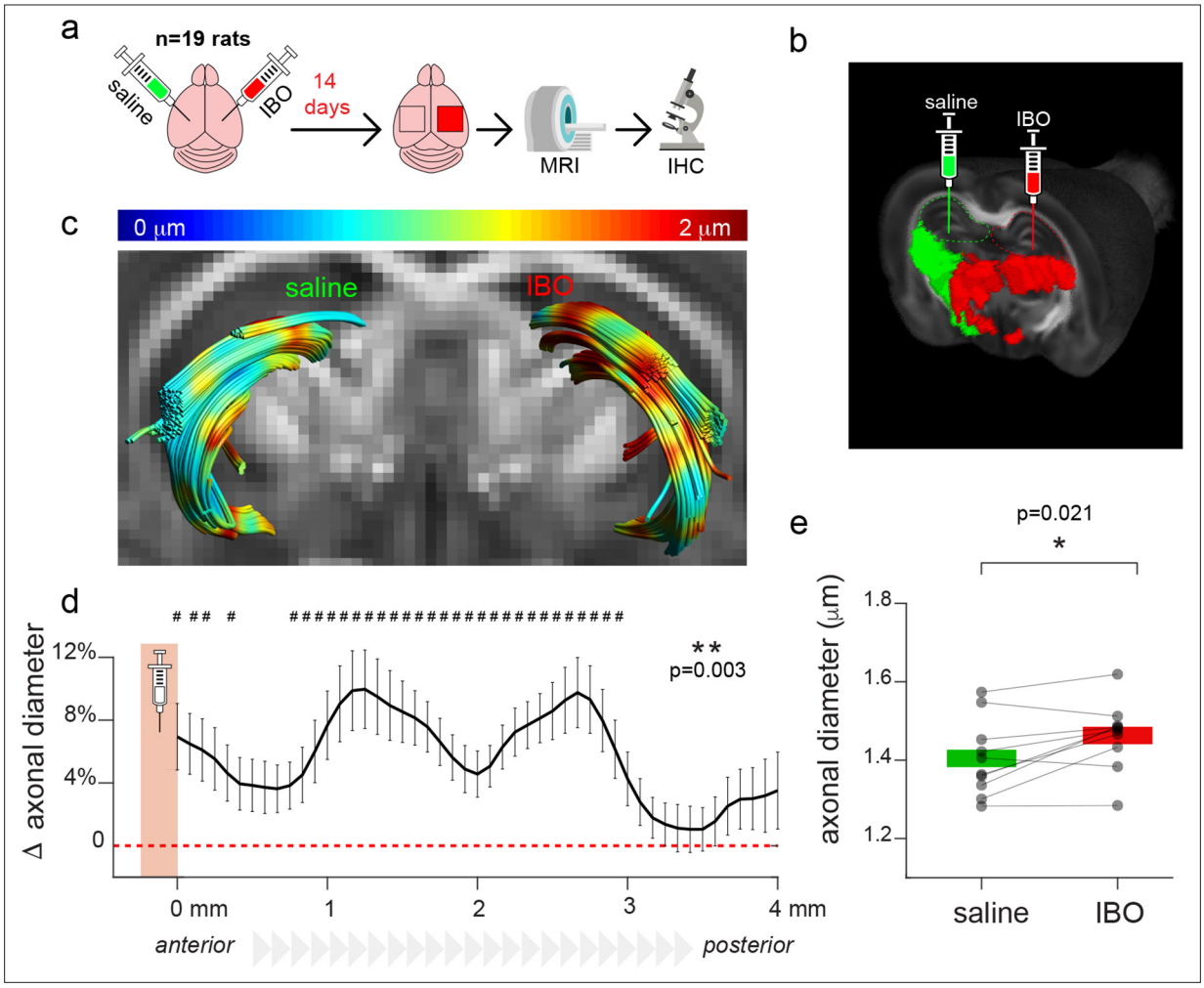


**Figure 1.** Experimental model of axonal damage. (**a**) Experimental scheme of stereotaxic injections of ibotenic acid (IBO) in the left hippocampus of n=19 rats. The right hippocampus was injected with saline solution and used as a control. (**b**) Visualization of the injection setup. (**c**) Example of the tractography of the fimbriae from one representative animal, superimposed on the fractional anisotropy map. The MRI axonal diameter proxy is projected on the tract through color coding. (**d**) Mean difference and standard deviation between groups of MRI axonal diameter proxy measured across all the streamlines constituting the fimbria in the antero-posterior axis, starting from the injection point (n=10). The injection site is shown in red. Asterisks represent significant group effect in the ANOVA, while hashtags represent significant post-hoc differences between groups in each location, corrected for multiple comparisons. (**e**) Mean MRI axonal diameter proxy calculated in the ibotenic vs saline-injected fimbria reconstructed using tractography. Asterisks represent significant differences (n=10, paired t test across hemispheres, p=0.021).

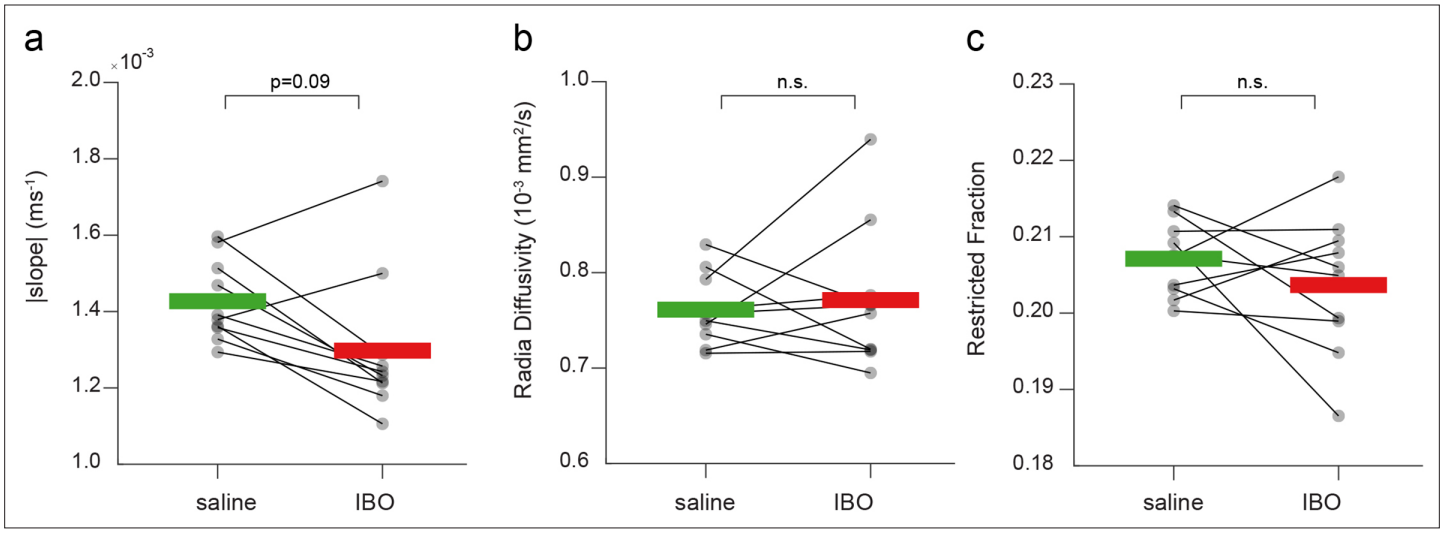


**Figure 1—figure supplement 1.** Other MRI parameters in control vs injected fimbriae. (**a**) Mean modulus of the slope of the dependency of the extra-axonal radial diffusivity from the diffusion time calculated in the ibotenic vs saline-injected fimbria reconstructed using tractography. The slope is always negative. (**b**) Extra-axonal radial diffusivity. (**c**) Restricted signal fraction. No significant differences are found (n=9, paired t test across hemispheres, p=0.09, 0.67 and 0.46 respectively).

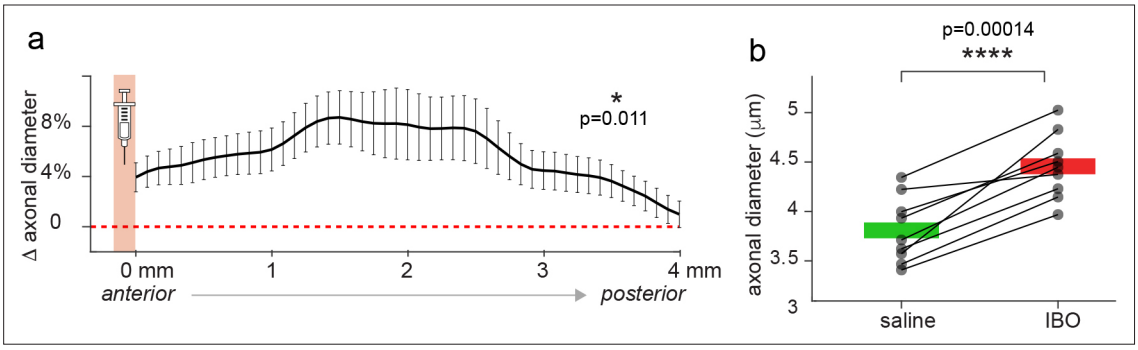


**Figure 1—figure supplement 2.** Axonal diameter estimation using the low b-value MRI protocol. (**a**) Mean difference and standard deviation between groups of axonal diameter measured across all the streamlines constituting the fimbria in the antero-posterior axis, starting from the injection point (n=9, low b-value protocol). The injection site is shown in red. Asterisk represents significant group effect in the ANOVA. (**b**) Mean MRI axonal diameter proxy calculated in the ibotenic vs saline-injected fimbria reconstructed using tractography. Asterisks represent significant differences (n=9, paired t test across hemispheres, p=0.000014).

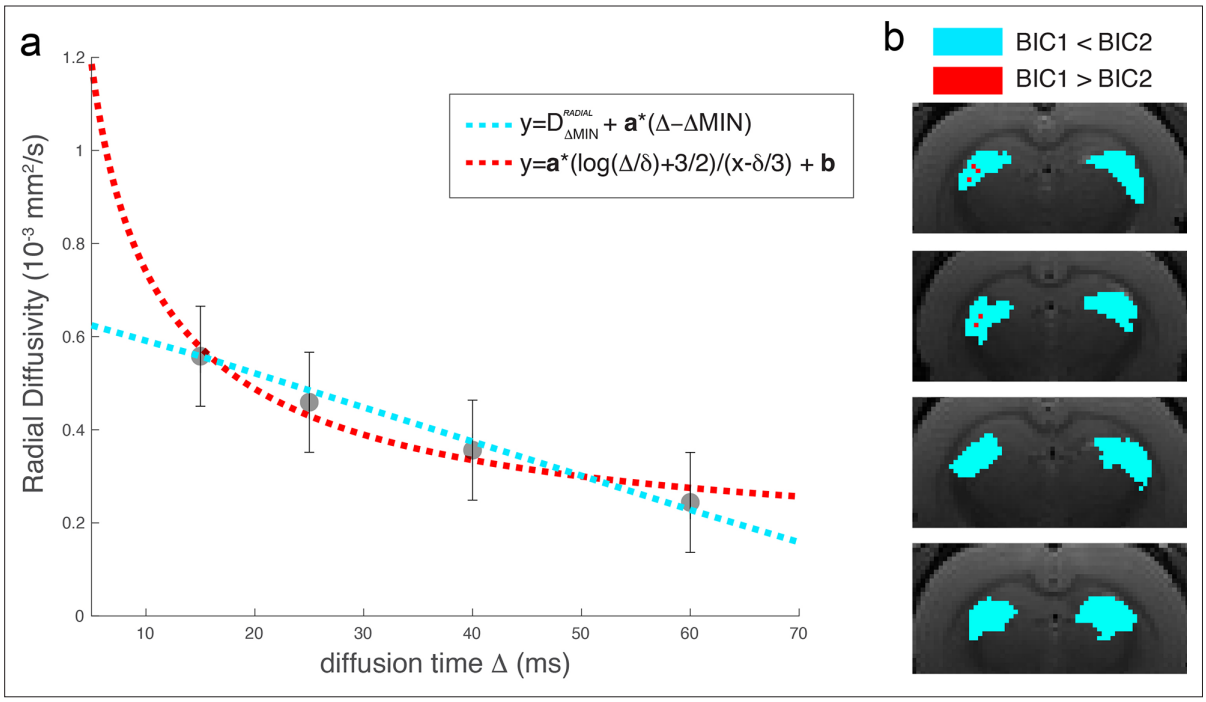


**Figure 1—figure supplement 3.** Comparison between linear and log(t)/t functional forms. (**a**) The two functional forms tested to fit the decay of the extra-axonal radial diffusivity are shown as a function of the diffusion times for the radial diffusivity measured on the protocol with lower b-value. (**b**) Example of the functional form chosen according to the BIC criterion in four of the animals.

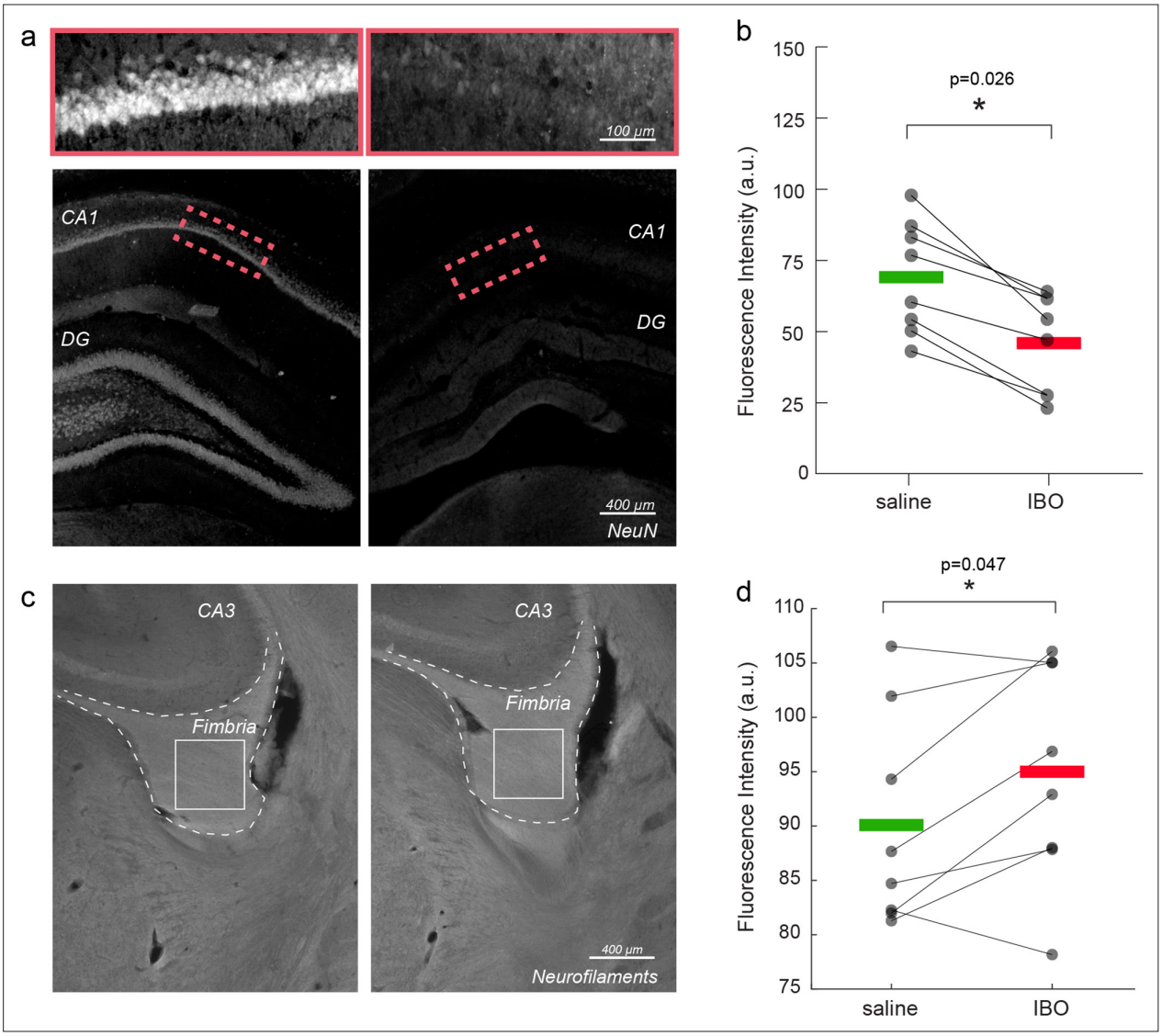


**Figure 2.** Immunofluorescence validation of axonal damage. (**a**) NeuN staining in control vs. injected hippocampi. (**b**) Mean NeuN intensity in control vs. injected hippocampi. Asterisks represent significant differences across hemispheres (n=8, paired t test, p=0.026). (**c**) Neurofilament staining in control vs. injected fimbria. (**d**) Mean neurofilament intensity in control vs. injected hippocampi. Asterisks represent significant differences in means across hemispheres (n=8, paired t test, p=0.047).

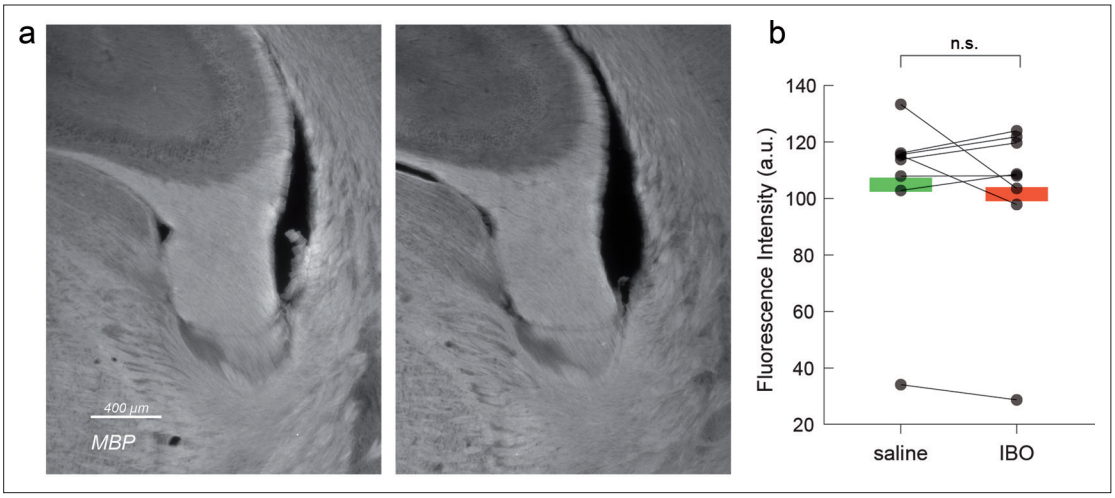


**Figure 2—figure supplement 1.** Myelin Basic Protein staining in injected versus control fimbria. (**a**) Myelin Basic Protein staining in injected versus control fimbria. (**b**) Mean Myelin Basic Protein intensity in control vs. injected hippocampi. No significant differences in myelination were found (n=8, paired t test, p=0.38).

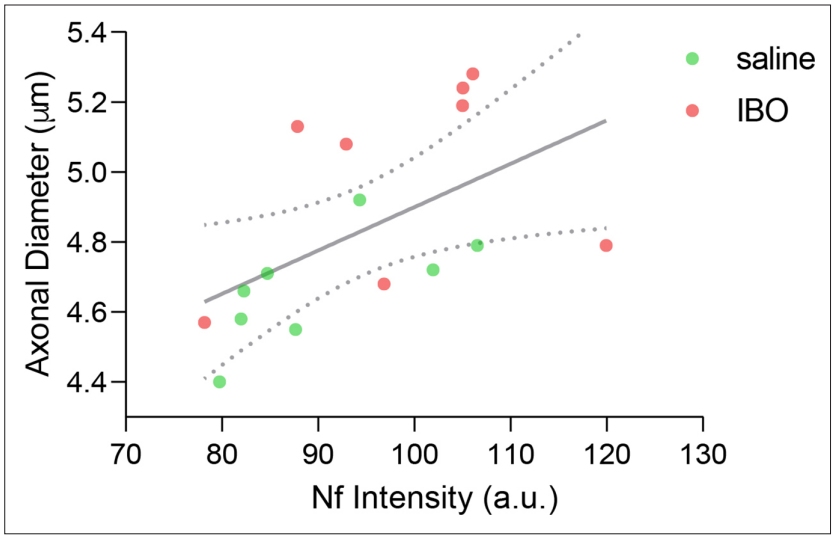


**Figure 2—figure supplement 2.** Correlation between MRI and histology. Significant correlation (*r*=0.54, p=0.029) between Neurofilaments fluorescence intensity and MRI axonal diameter proxy measured with the AxCaliber model for all hemispheres in the fimbria. Ibotenic acid injected hemispheres are shown in red and saline injected are shown in green.

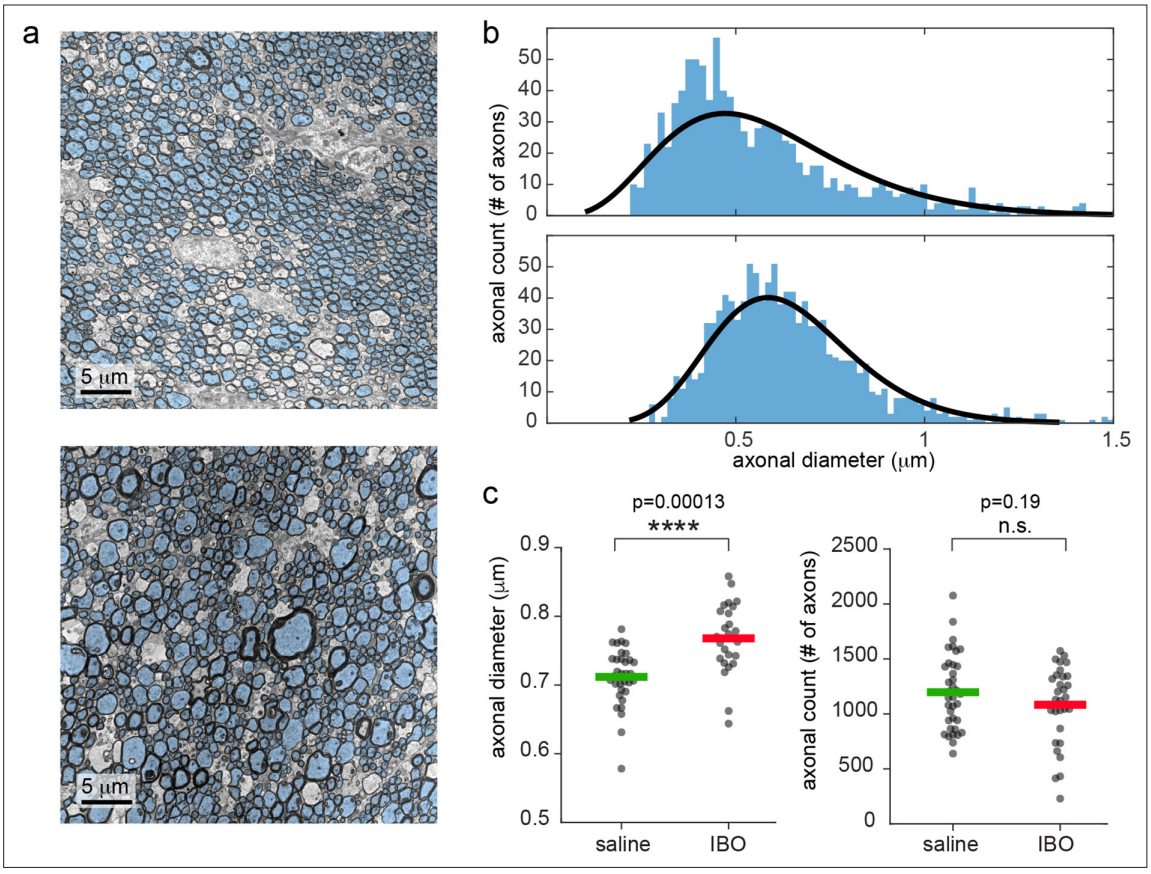


**Figure 3.** Electron microscopy shows increased mean axonal diameter in ibotenic-injected hemisphere compared to saline. (**a**) Representative STEM photos for saline and ibotenic acid fimbriae. Segmented axons are overlaid in light blue. (**b**) Histogram of the axonal count in one representative animal: upper line, saline injected, lower line, ibotenic. Black lines represent the gamma function better fitting the histogram. (**c**) Mean axonal diameter (left) and count (right) in each photo and group. Asterisks represent significant unpaired t test differences between groups for axonal diameter (n=6, p=0.00013).

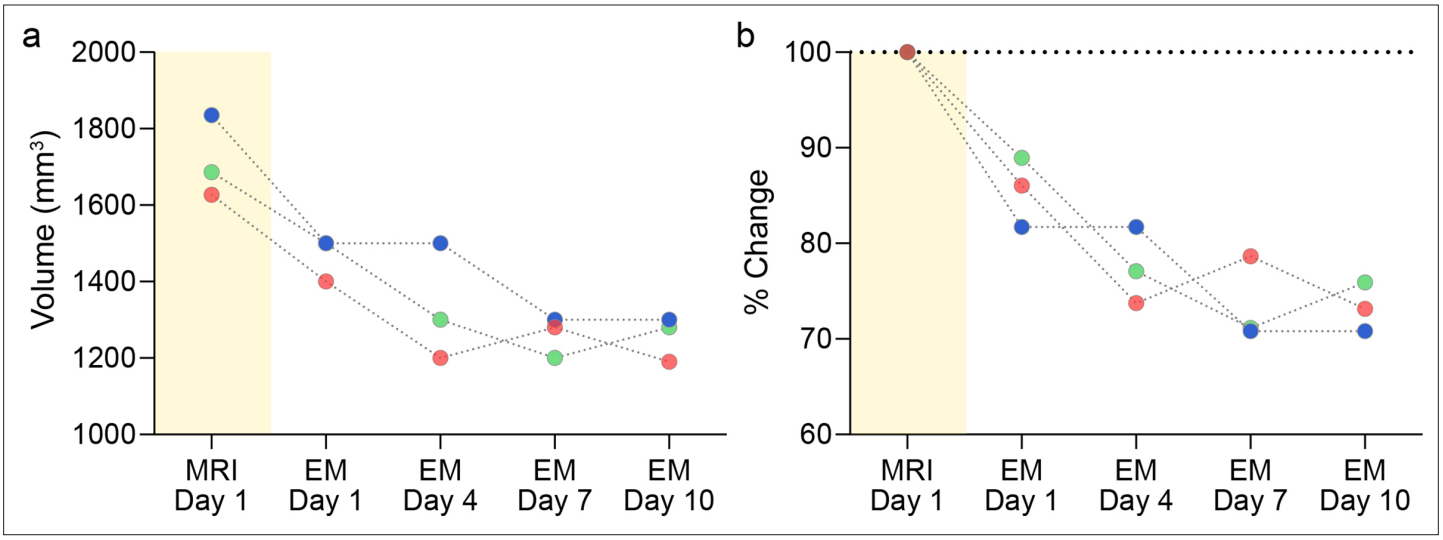


**Figure 3—figure supplement 1.** Brain shrinkage during histology. (**a**) Brain volume quantification in mm obtained for three animals in vivo through manual segmentation of MRI images, and post-perfusion at days 1, 4, 7, and 10 while embedded in the fixative (2% paraformaldehyde and 2.5% glutaraldehyde in 0.1 M cacodylate buffer). (**b**) Same, but relative to in vivo volume.

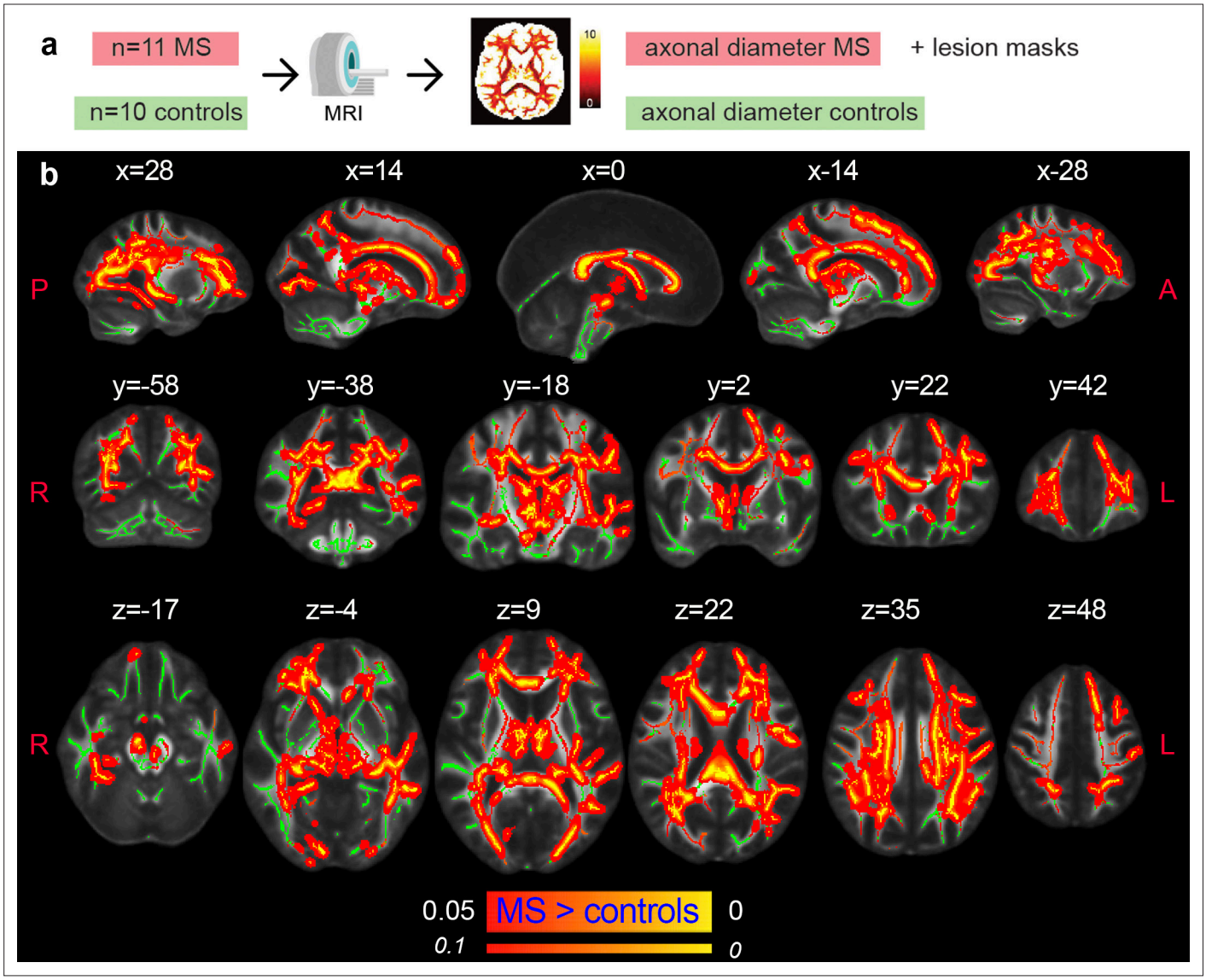


**Figure 4.** Axonal damage in MS normal-appearing white matter. (**a**) Experimental scheme. (**b**) Tract-based spatial statistics showing voxels in which the mean MRI axonal diameter proxy is significantly increased in multiple sclerosis versus healthy conditions (n=21, p<0.05, corrected). The opposite contrast was not statistically significant. Green: skeletonized white matter. Inflated red-yellow (through the pipeline tbss_fill): significant p value. Red-yellow: p-value <0.1.

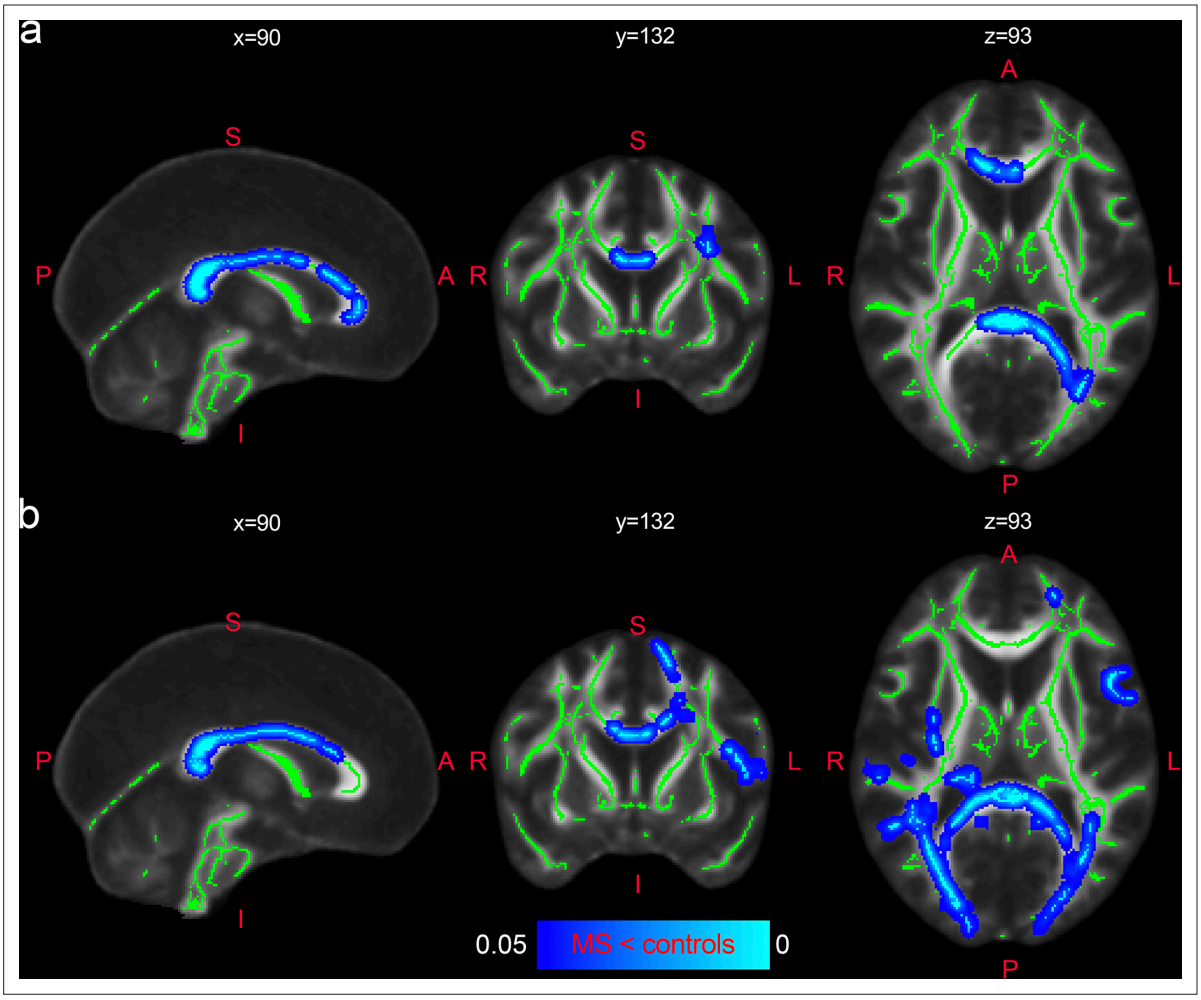


**Figure 4—figure supplement 1.** Slope of extra-axonal radial diffusivity and restricted signal fraction in patients vs. controls. Tract-based spatial statistics showing voxels in which the slope of the extra-axonal radial diffusivity decay for increasing diffusion time (panel **a**) and the restricted signal fraction (panel **b**) are significantly decreased in multiple sclerosis versus healthy conditions (n=21, p<0.05, corrected). The opposite contrast was not statistically significant. Green: skeletonized white matter. Inflated blue-lighblue (through the tbss_fill pipeline): significant p-value.

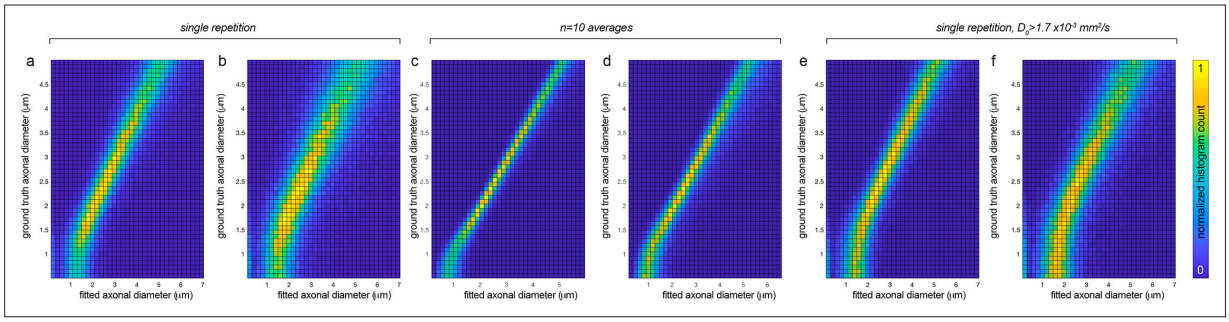


**Figure 4—figure supplement 2.** Rician simulations showing accuracy of MRI axonal diameters proxy. Normalized 2-D histograms of fitted versus ground truth axonal diameters for two SNRs matching human (panel **a**) and animal (panel **b**) data for a single Rician noise realization, and averaged over 10 repetitions (panels **c** and **d**). In panel **e** and **f**, the simulations are repeated with intra-axonal axial diffusivity range 1.7–2.2x10$^{-3}$ mm$^2$/s for a single Rician noise realization.

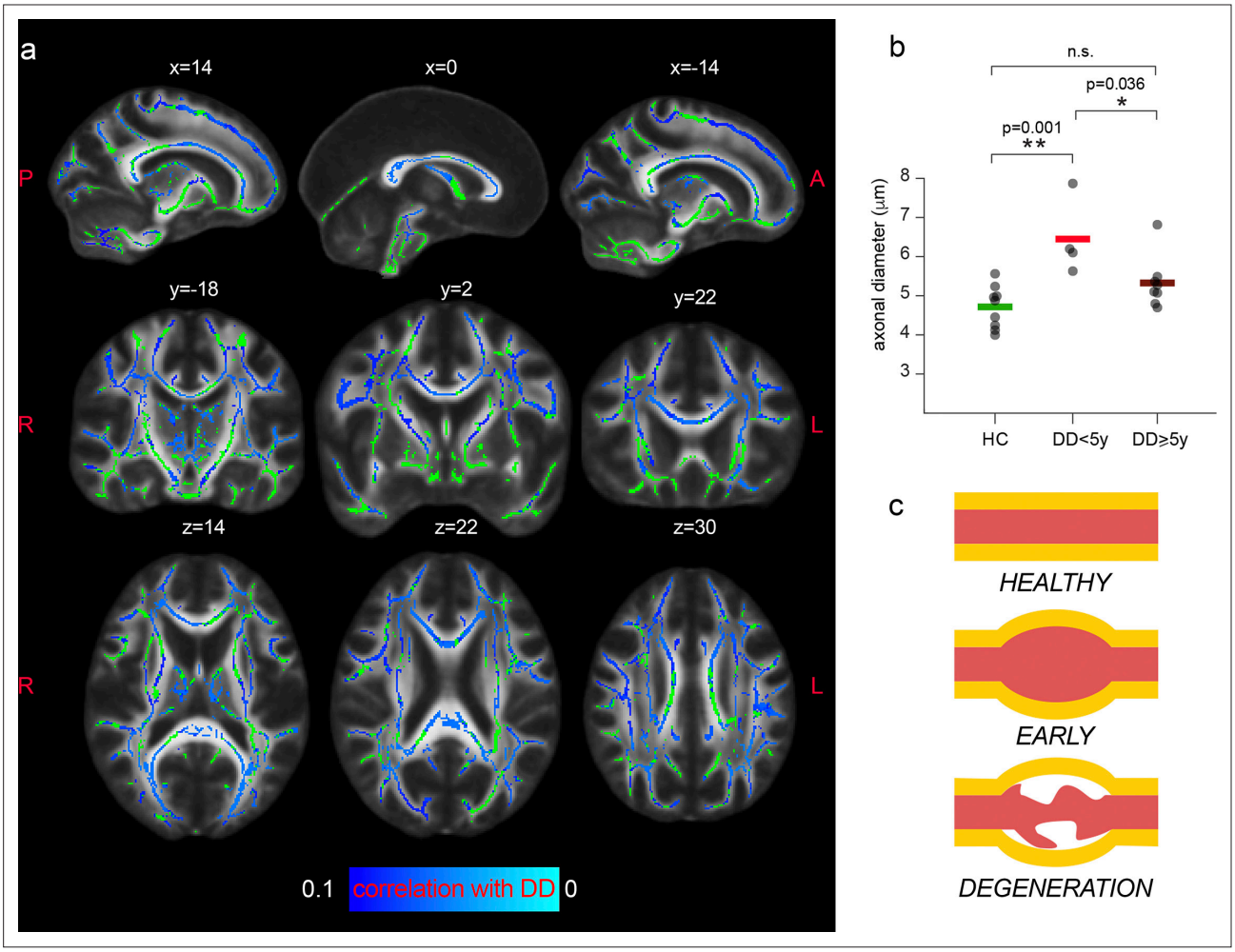


**Figure 5.** Axonal diameter is preferentially increased in patients with early MS. (**a**) Tract-based spatial statistics showing voxels in which a trend of negative association between the MRI axonal diameter proxy and the disease duration (DD) in patients is present (n=11, p<0.1; lowest p-value = 0.051 corrected). Green: skeletonized white matter. Bluel-light blue: p value. (**b**) Mean axonal diameter in the whole with matter of healthy controls (n=10, green), MS patients early in the disease course (n=4, <5 years, in red) and MS patients with a longer disease trajectory (n=7, ≥ 5 years, dark red). Asterisks represent unpaired post-hoc group differences following significant group effect in the ANOVA. (**c**) Schematic progression of early axonal damage. Figure 5c has been adapted from Figure 1E from ***Luchicchi et al., 2021***.